Supplementary Information

Highly dispersed Co nanoparticles decorated on N-doped defective carbon nano-framework for hybrid Na-Air battery

Jingyi Zhu[a#], Tao Qu[a, b#], Fengmei Su[a], Yuqi Wu[a], Yao Kang[c,*], Kunfeng Chen[d], YaochunYao[a], Wenhui Ma[a], Bing Yang[a], Yongnian Dai[a], Feng Liang[a,b,*], Dongfeng Xue[d]

[a] Faculty of Metallurgical and Energy Engineering, Kunming University of Science and Technology, Kunming 650093, China

[b] State Key Laboratory of Complex Nonferrous Metal Resources Clean Utilization, Kunming University of Science and Technology, Kunming 650093, China

[c] Institute of Applied Physics and Materials Engineering, University of Macau, Avenida da Universidade, Taipa, Macau, China

[d] State Key Laboratory of Rare earth Resources Utilization, Chinese Academy of Science, Changchun 130022, China

(#The contributions of Jingyi Zhu and Tao Qu are equal and are the first authors.)

Table S1. Performance of bifunctional catalysts derived from Co-MOF for ORR and OER.

Catalysts	Electrolyte	Onset Potential (V)	Half-wave potential (V)	J at 1.6 V (mA cm^{-2})	Ref.
BNPC-1100	0.1 M KOH	0.894	0.793	4.7	[1]
Co@N-CNTF-2	0.1 M KOH	0.91	0.81	10	[2]
CoZn-NC-700	0.1 M KOH	0.97	0.84	6.0	[3]
MnO@Co/N-C	0.1 M KOH	0.88	0.83	2.4	[4]
Co-CoP-HNC	0.1 M KOH	0.94	0.83	140	[5]
Co-CoO-C	0.1 M KOH	0.90	0.82	4.0	[6]
Co-N-C-0	0.1 M KOH	0.85	0.81	1.5	Present work
Co-N-C-0.2	0.1 M KOH	0.87	0.80	2.5	Present work
Co-N-C-0.5	0.1 M KOH	0.92	0.82	4.4	Present work

Table S2. The atomic percentage of fitted peaks of N 1s in Co-N-C catalysts

Catalysts	Pyridinc N (at %)	Pyrrolic N (at %)	CoN_x (at %)
Co-N-C-0	0.13	0.09	0.11
Co-N-C-0.2	0.08	0.17	0.13
Co-N-C-0.5	0.14	0.13	0.30

Table S3. Atomic ratio of Co^{3+}, Co^{2+}, and Co^{0} in Co-N-C catalysts calculated by XPS

Catalysts	Co^{3+} (at %)	Co^{2+} (at %)	Co^{0} (at %)
Co-N-C-0	0.06	0.06	0.01
Co-N-C-0.2	0.07	0.05	0.01
Co-N-C-0.5	0.07	0.02	0.01

Table S4. Discharge–charge performance of hybrid sodium-air batteries with different catalysts

Catalysts	Discharge voltage (V)	Charge voltage (V)	Voltage gap (V)	Current densities	Roundtrip efficiency (%)	Ref.
Mn_3O_4/C	2.60	3.51	0.91	1 mA·cm^{-2}	74.07	[7]
$Co_3(PO_4)_2$	2.82	3.41	0.59	0.01 mA·cm^{-2}	82.70	[8]
dp-$MnCo_2O_4$/N-rGO	2.75	3.14	0.39	0.13 mA·cm^{-2}	87.58	[9]
Pt/C	2.85	3.38	0.53	0.025 mA·cm^{-2}	84.32	[10]
Carbon paper	2.6	3.59	0.99	0.025 mA·cm^{-2}	72.42	[10]
Carambola-shaped VO_2	2.81	3.45	0.64	0.01 mA·cm^{-2}	81.45	[11]
Pt/C	2.94	3.55	0.61	0.01 mA·cm^{-2}	82.82	[11]
Pt/C	2.69	3.20	0.51	0.1 mA·cm^{-2}	84.06	Present work
Co-N-C-0	2.60	3.17	0.57	0.1 mA·cm^{-2}	82.02	Present work

Co-N-C-0.2	2.79	3.12	0.33	0.1 mA·cm^{-2}	89.42	Present work
Co-N-C-0.5	2.80	3.11	0.38	0.1 mA·cm^{-2}	90.03	Present work

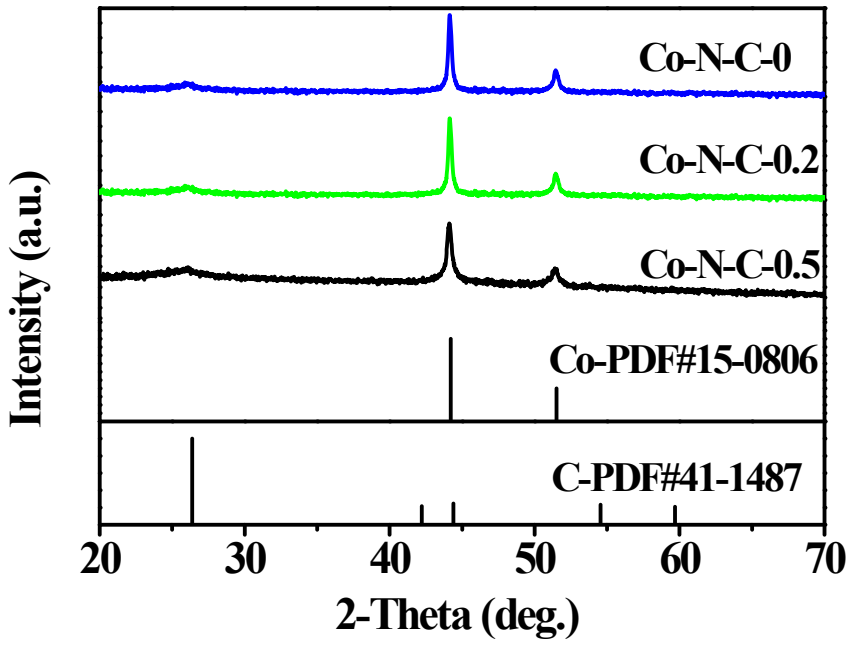

Figure S1. XRD patterns of Co-N-C-0, Co-N-C-0.2, and Co-N-C-0.5.

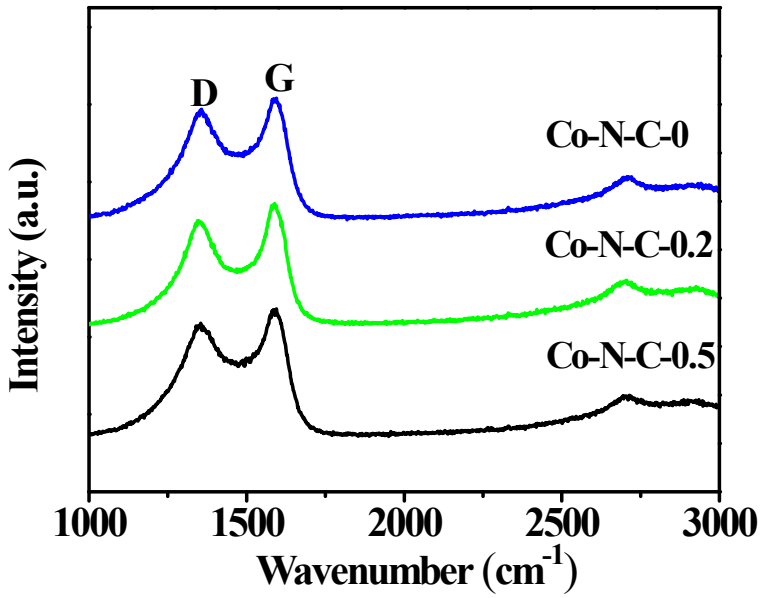

Figure S2. Raman spectra of Co-N-C-0, Co-N-C-0.2, and Co-N-C-0.5.

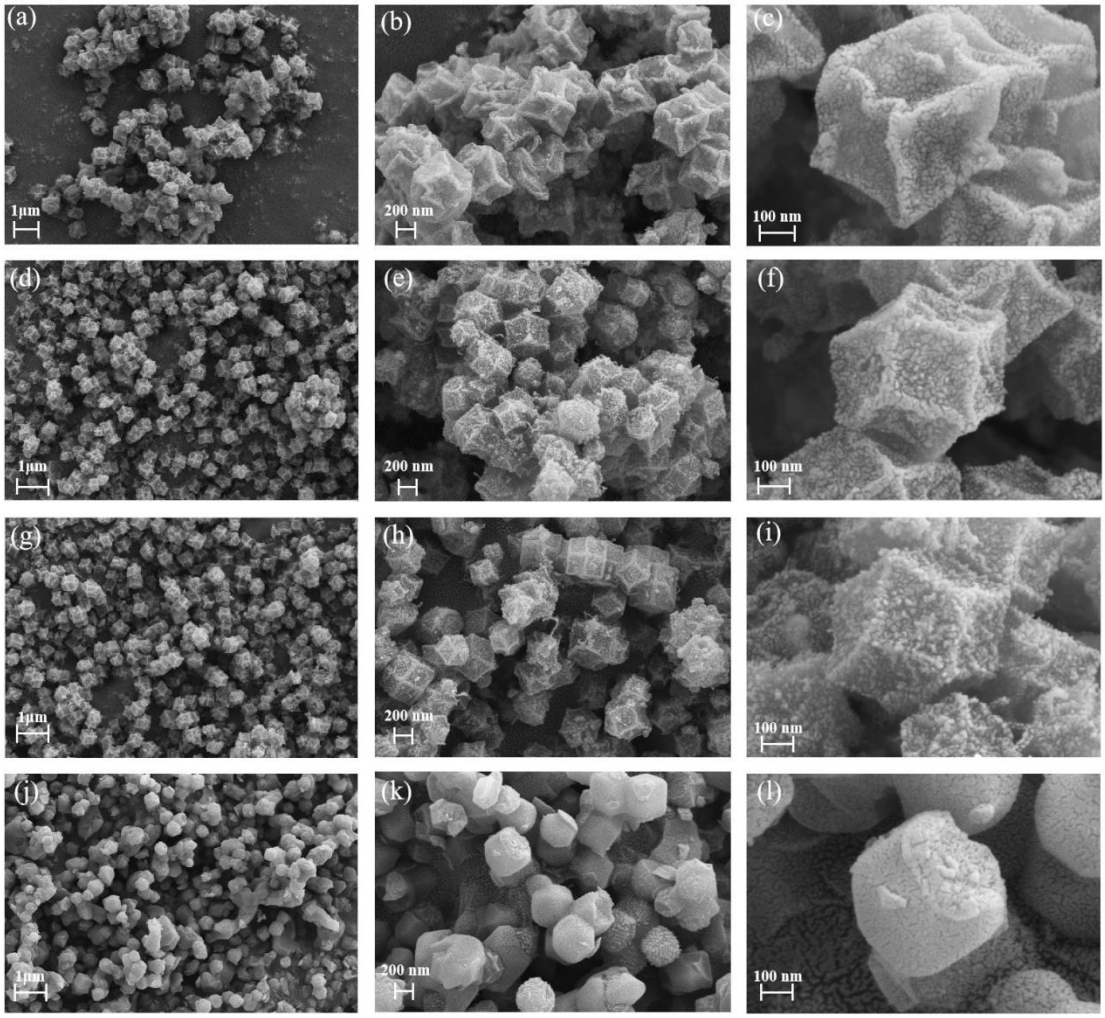

Figure S3. FESEM images of (a, b, c) Co-N-C-0; (d, e, f) Co-N-C-0.2; (g, h, i) Co-N-C-0.5; (j, k, l) Co-N-C-1.0.

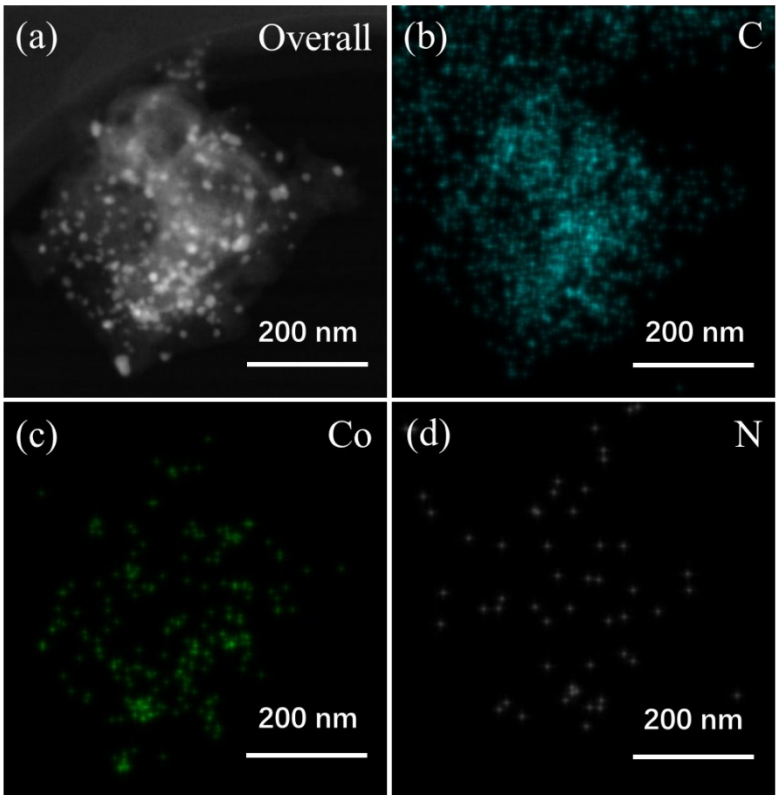

Figure S4. EDS elemental maps of Co-N-C-0.5.

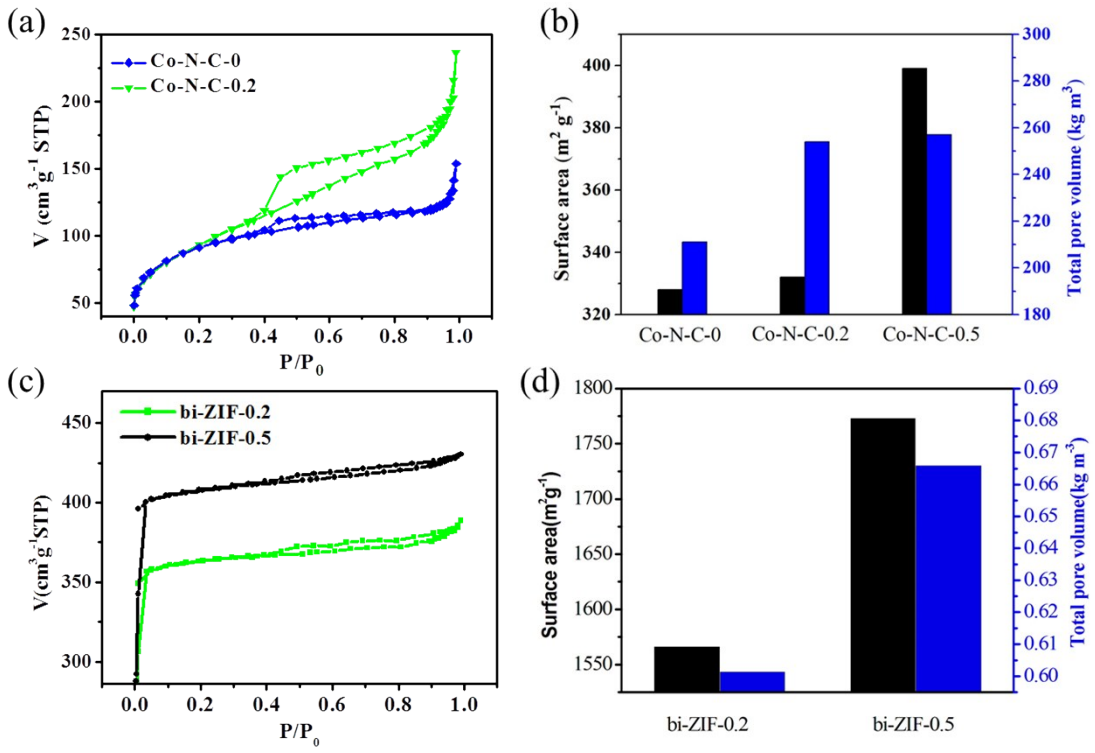

Figure S5. (a) N_2 adsorption-desorption isotherms of Co-N-C-0 and Co-N-C-0.2; (b) surface area and total pore volume of Co-N-C-0, Co-N-C-0.2, and Co-N-C-0.5; (c) N_2 adsorption-desorption isotherms of bi-ZIF-0.2 and bi-ZIF-0.5; (d) surface area and total pore volume of bi-ZIF-0.2 and bi-ZIF-0.5.

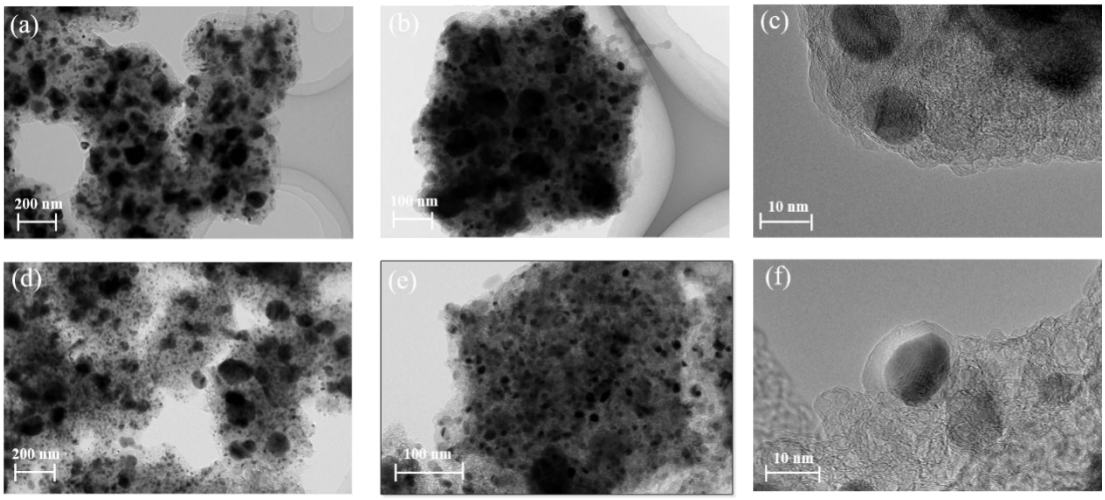

Figure S6. TEM images of (a,b,c) Co-N-C-0 and (d,e,f) Co-N-C-0.2.

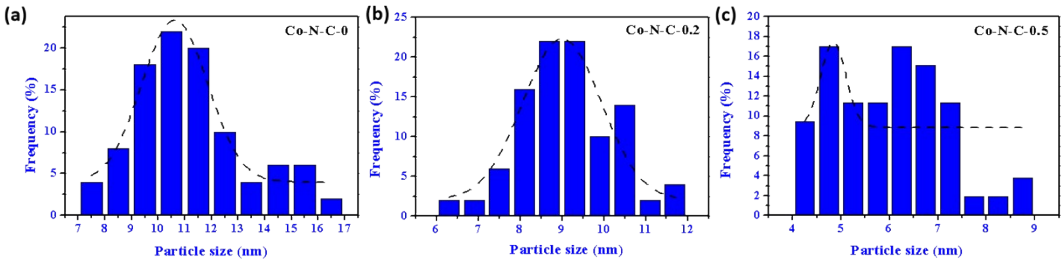

Figure S7. The size distribution of (a) Co-N-C-0; (b) Co-N-C-0.2; (c) Co-N-C-0.5.

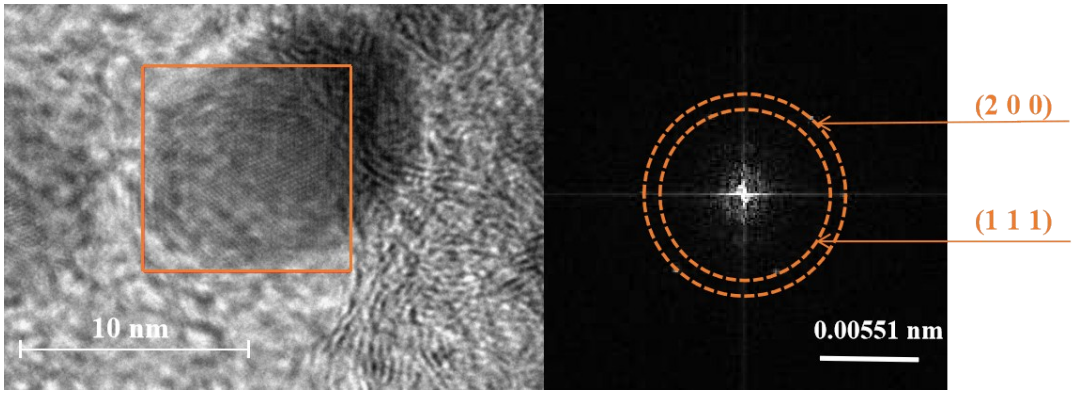

Figure S8. SAED of Co-N-C-0.5

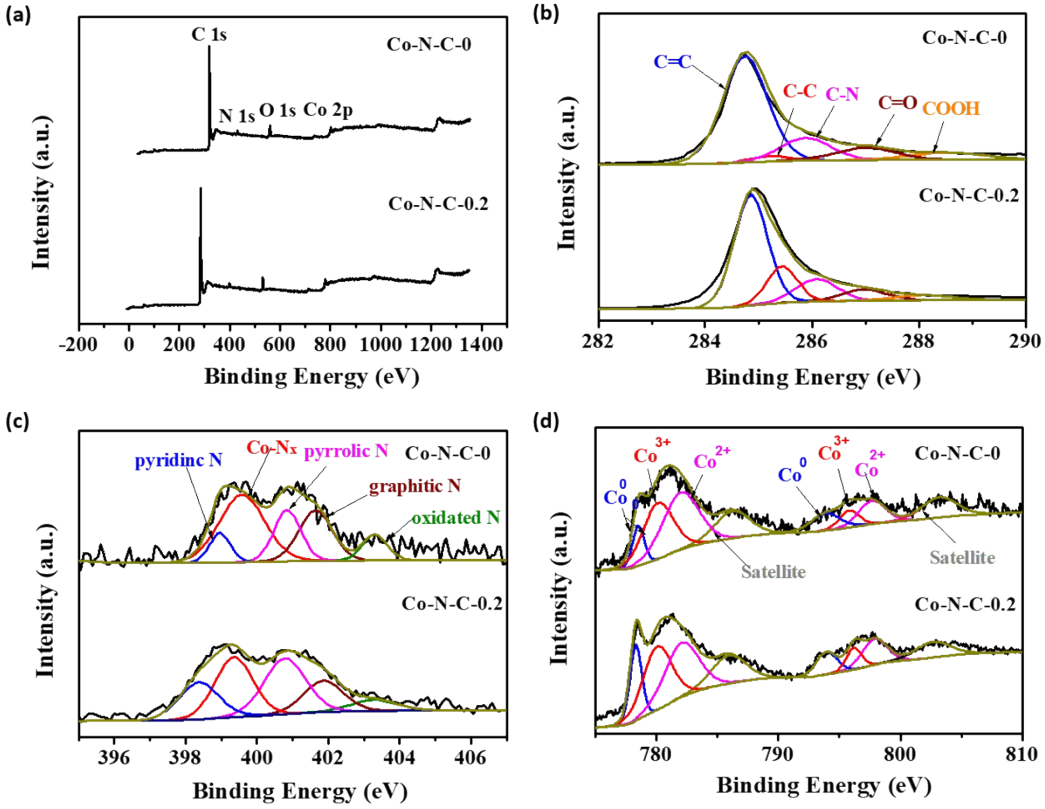

Figure S9. (a) XPS survey spectra and high−resolution spectra of (b) C 1s, (c) N 1s and (d) Co 2p of Co−N−C−0 and Co−N−C−0.5 catalysts.

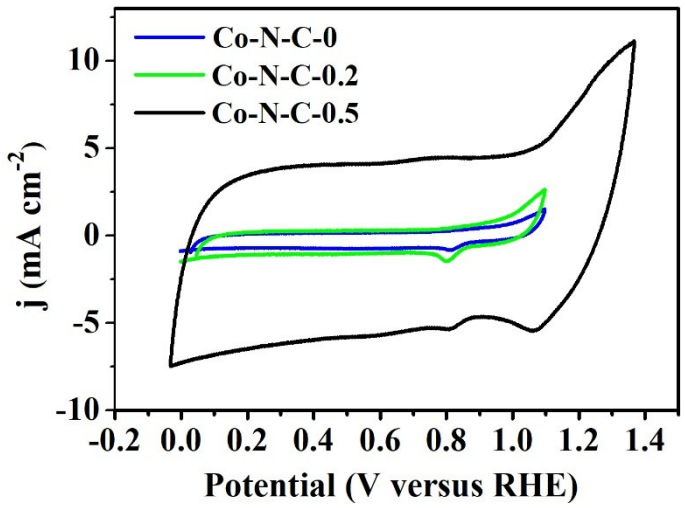

Figure S10. CV curves of different catalysts.

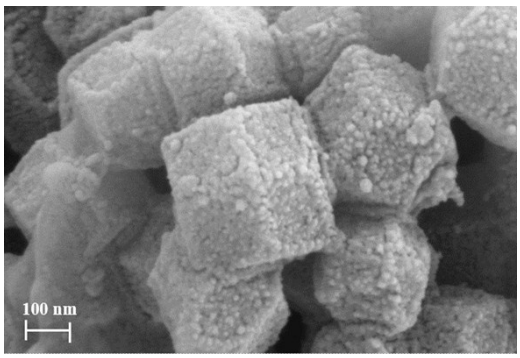

Figure S11. FESEM images of Co-N-C-0.5 after 20 cycles.

Reference

[1] Qian Y , Hu Z , Ge X , et al. A metal-free ORR/OER bifunctional electrocatalyst derived from metal-organic frameworks for rechargeable Zn-Air batteries[J]. Carbon, 2017, 111:641-650.

[2] Guo H , Feng Q , Zhu J , et al. Cobalt nanoparticle-embedded nitrogen-doped carbon/carbon nanotube frameworks derived from metal-organic framework for tri-functional ORR, OER and HER electrocatalysis[J]. Journal of Materials Chemistry A, 2019, 7(8):3664-3672.

[3] Chen B, He X, Yin F, et al. MO-Co@ N-doped carbon (M= Zn or Co): vital roles of inactive Zn and highly efficient activity toward oxygen reduction/evolution reactions for rechargeable Zn-Air battery[J]. Advanced Functional Materials, 2017, 27(37): 1700795.

[4] Chen Y , Guo Y , Cui H , et al. Bifunctional electrocatalysts of MOF-derived Co-N/C on bamboo-like MnO nanowires for high-performance liquid and solid-state Zn-air batteries[J]. Journal of Materials Chemistry A, 2018, 6(20): 9716-9722.

[5] Hao Y, Xu Y, Liu W, et al. Co/CoP embedded in a hairy nitrogen-doped carbon polyhedron as an advanced tri-functional electrocatalyst[J]. Materials Horizons, 2018, 5(1): 108-115.

[6] Lu H S, Zhang H, Zhang X, et al. Transformation of carbon-encapsulated metallic Co into ultrafine Co/CoO nanoparticles exposed on N-doped graphitic carbon for high-performance rechargeable zinc-air battery[J]. Applied Surface Science, 2018, 448: 369-379.

[7] Liang F, Hayashi K. A High-Energy-Density Mixed-Aprotic-Aqueous Sodium-Air Cell with a Ceramic Separator and a Porous Carbon Electrode[J]. Journal of the Electrochemical Society, 2015, 162(7): A1215-A1219.

[8] Senthilkumar B, Khan Z, Park S, et al. Exploration of cobalt phosphate as a potential catalyst for rechargeable aqueous sodium-air battery[J]. Journal of Power Sources, 2016, 311:29-34.

[9] Kang Y, Zou D, Zhang J, et al. Dual–phase Spinel $MnCo_2O_4$ Nanocrystals with Nitrogen-doped Reduced Graphene Oxide as Potential Catalyst for Hybrid Na-Air Batteries[J]. Electrochimica Acta, 2017, 244:222-229.

[10] Sahgong S H, Senthilkumar S T, Kim K, et al. Rechargeable aqueous Na-air batteries: Highly improved voltage efficiency by use of catalysts[J]. Electrochemistry Communications, 2015, 61: 53-56.

[11] Khan Z, Senthilkumar B, Park S O, et al. Carambola-shaped VO_2 nanostructures: a binder-free air electrode for an aqueous Na-air battery[J]. Journal of Materials Chemistry A, 2017, 5(5): 2037-2044.